J. Chem. Eng. Data **2003,** *48,* 603−607

Adsorption Equilibria of Methane, Ethane, Ethylene, Nitrogen, and Hydrogen onto Activated Carbon

Byoung-Uk Choi,* Dae-Ki Choi, Young-Whan Lee, and Byung-Kwon Lee

CFC Alternatives Research Center, Korea Institute of Science & Technology, P.O. Box 131,
Cheongryang, Seoul 130-650, Korea

Sung-Hyun Kim

Department of Chemical Engineering, Korea University, Seoul 136-701, Korea

---

Adsorption equilibria of single components for pure methane, ethane, ethylene, hydrogen, and nitrogen onto activated carbon adsorbent (Calgon Co.) were measured. The results were obtained with a static volumetric method at 293.15 K, 303.15 K, and 313.15 K and at pressures up to 2 MPa. Experimental data were correlated by the Langmuir−Freundlich equation. Isosteric enthalpies of adsorption were calculated and shown according to surface loading.

Introduction

Recent demands for hydrogen for utilization in such fields as fuel cells, semiconductor processing, and the petrochemical industry are increasing. Also, hydrogen is regarded as an ecologically clean and renewable energy source. Most industrial hydrogen has been produced from steam reforming of light hydrocarbon, partial oxidation of heavy hydrocarbon, recovery from coke oven gas, water electrolysis, and so forth. Recently, natural gas pyrolysis and plasma reaction processes have been studied to produce CO_2-free hydrogen. Although they do not emit carbon dioxide, a separation technology to separate high purity hydrogen is still required, since impurities still remain in their products.

There are several methods for hydrogen recovery and purification. The adsorption process has been generally recognized as low in energy consumption with the added advantage of having very precise (99.999%, H_2) component separation using pore size and surface characteristics of the adsorbent.[1,2] Thus, the main advantages of adsorption, compared with other separation techniques, are the high selectivity and the relatively high capacity of the adsorbents.[3] Especially, the pressure swing adsorption technology is attractive for its low energy requirements and low capital investment costs. Many sophisticated pressure swing adsorption processes have been developed and commercialized since the introduction of the Skarstrom cycle.[4] In fact, there has been a lot of research on separation of hydrogen using pressure swing adsorption process.[5−8]

High-pressure range single-component and multicomponent adsorption equilibrium data are needed to separate some components using the pressure swing adsorption process. However, due to the substantial amount of time involved in conducting related experiments, there is scant published data on the mixtures.[9] The mixture isotherm data are not usually obtained directly, but through correlated single-component isotherms.[10] Some researchers used only single-component adsorption data to predict multicomponent adsorption behavior.[2,9,11−13] So, it is necessary to measure exact single-component adsorption equilibrium data.

Table 1. Characteristics of Activated Carbon Adsorbent

type	PCB
nominal pellet size/mesh	6−16
average pellet size/mm	0.115
BET surface area/$m^2 \cdot g^{-1}$	1150−1250
bulk density/$g \cdot cm^{-3}$	0.44
total pore volume/$cm^3 \cdot g^{-1}$	0.72

Presented in this paper are the adsorption equilibria of the single components for methane and hydrogen, the main products of natural gas pyrolysis, and the minor products for ethane, ethylene, and nitrogen, onto activated carbon adsorbent. Measurements of adsorption equilibrium data were made at assorted temperatures and pressures, namely, at 293.15 K, 303.15 K, and 313.15 K and at pressures up to 2 MPa. Experimental data were correlated by the Langmuir−Freundlich equation.

Experimental Section

Materials. Activated carbon (Calgon Co.) was chosen as an adsorbent. The physical properties, as tabulated in Table 1, were obtained from the manufacturer's report. Prior to measurement, the adsorbent was maintained at 423.15 K in a drying vacuum oven for more than 12 h to remove impurities. The adsorbates, and their purities, were methane (99.9%), ethane (99.5%), ethylene (99%), hydrogen (99.9%), and nitrogen (99.999%).

Apparatus and Procedure. The adsorption apparatus shown in Figure 1 is based on the static volumetric method. There are a reaction cell and a loading cell. Used were $^1/_8$ in. tubes and $^1/_8$ in. valves to minimize dead volume as much as possible. The reaction cell volume was 521.61 ± 1 mL; the loading cell volume, 522.73 ± 1 mL. The reaction cell, loading cell, and dead volumes were measured using helium gas. The total amount of vapor introduced and recovered in the system was determined by appropriate pressure, temperature, and volume measurements. The temperature in each cell was measured by K-type thermocouple operated within ±0.01 K accuracy; the pressure was measured with a pressure transducer. Temperatures and pres-

---

* To whom correspondence should be addressed. E-mail: ares76@kist.re.kr. Fax number: +82-2-958-5809.

10.1021/je020161d CCC: $25.00

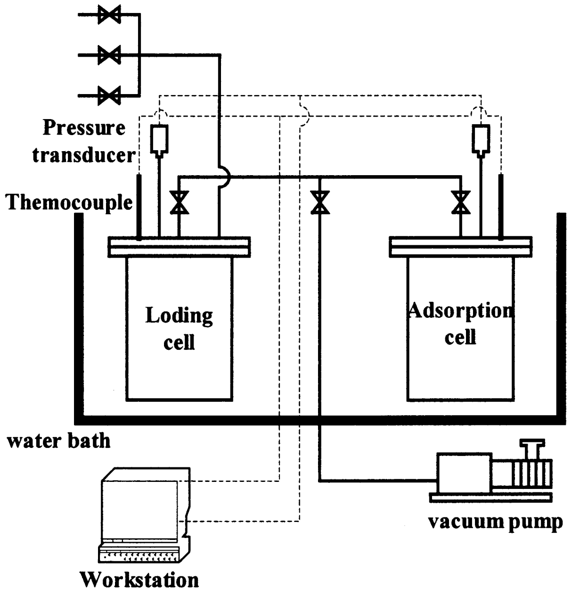

Figure 1. Schematic diagram of the adsorption apparatus.

Table 2. Adsorption Isotherm Data for CH_4 onto Activated Carbon

293.15 K		303.15 K		313.15 K	
P	q	P	q	P	q
kPa	mol·kg^{-1}	kPa	mol·kg^{-1}	kPa	mol·kg^{-1}
48.401	0.298	45.697	0.234	60.206	0.188
79.890	0.639	77.272	0.505	88.212	0.423
120.320	1.003	115.194	0.815	130.777	0.684
166.450	1.337	163.991	1.067	170.513	0.950
217.572	1.633	213.210	1.339	217.192	1.189
270.235	1.902	286.532	1.659	288.153	1.484
324.072	2.114	369.893	1.956	377.285	1.779
398.549	2.385	464.182	2.257	470.148	2.045
484.913	2.653	605.909	2.610	614.711	2.389
626.898	3.022	779.190	2.946	784.580	2.712
796.948	3.360	970.694	3.244	971.893	2.996
987.771	3.665	1175.918	3.501	1171.605	3.253
1188.653	3.913	1377.258	3.707	1379.935	3.464
1381.295	4.110	1568.584	3.877	1560.303	3.611
1549.662	4.256				
D		D		D	
0.000 399		0.000 376		0.000 613	

Table 3. Adsorption Isotherm Data for C_2H_6 onto Activated Carbon

293.15 K		303.15 K		313.15 K	
P	q	P	q	P	q
kPa	mol·kg^{-1}	kPa	mol·kg^{-1}	kPa	mol·kg^{-1}
23.529	1.156	33.009	1.169	33.411	1.071
51.649	2.788	60.696	2.349	73.655	2.463
129.183	4.258	134.519	3.750	160.329	3.604
265.044	5.107	262.477	4.626	292.147	4.387
410.275	5.534	409.026	5.076	432.411	4.796
592.295	5.802	523.476	5.388	616.031	5.119
797.306	5.948	800.773	5.577	818.093	5.338
999.820	6.031	1067.939	5.695	1026.441	5.421
1272.845	6.032	1450.168	5.716	1284.072	5.496
D		D		D	
0.0217		0.0185		0.0177	

sures were recorded at constant time intervals with a mobile recorder (MV100, Yokogawa Co.). During adsorption, the loading cell, the reaction cell, and all lines were immersed in a water bath (SWB-20, Jeio tech.) maintained at ±0.02 K via a refrigeration circulator (RBC-11, Jeio tech.).

Table 4. Adsorption Isotherm Data for C_2H_4 onto Activated Carbon

293.15 K		303.15 K		313.15 K	
P	q	P	q	P	q
kPa	mol·kg^{-1}	kPa	mol·kg^{-1}	kPa	mol·kg^{-1}
34.730	1.368	54.823	0.972	57.157	0.823
74.133	2.872	166.391	3.431	169.800	3.101
161.678	4.153	277.913	4.305	285.991	3.944
286.600	4.955	406.425	4.849	420.977	4.493
416.454	5.410	533.515	5.199	547.981	4.827
594.993	5.779	668.357	5.451	671.816	5.048
794.171	6.027	799.116	5.623	785.653	5.218
1001.472	6.214	908.520	5.730	906.881	5.359
1208.972	6.295	1009.235	5.812	1022.847	5.455
1404.543	6.357	1161.088	5.919	1169.862	5.550
1674.430	6.376	1333.150	6.026	1351.392	5.638
		1514.121	6.081	1522.794	5.700
		1623.229	6.088	1617.985	5.734
D		D		D	
0.0167		0.0165		0.0197	

Table 5. Adsorption Isotherm Data for N_2 onto Activated Carbon

293.15 K		303.15 K		313.15 K	
P	q	P	q	P	q
kPa	mol·kg^{-1}	kPa	mol·kg^{-1}	kPa	mol·kg^{-1}
123.023	0.325	110.197	0.264	121.062	0.204
221.382	0.592	200.200	0.487	219.513	0.387
324.400	0.823	300.436	0.687	328.548	0.577
427.666	1.011	401.220	0.863	471.747	0.796
544.902	1.198	517.833	1.039	660.269	1.036
693.258	1.411	692.645	1.266	863.883	1.243
863.266	1.611	950.921	1.531	1081.473	1.419
1050.721	1.791	1239.527	1.769	1342.119	1.583
1294.690	1.980	1542.180	1.966	1629.274	1.722
1574.435	2.171				
D		D		D	
0.00882		0.00934		0.0129	

Table 6. Adsorption Isotherm Data for H_2 onto Activated Carbon

293.15 K		303.15 K		313.15 K	
P	q	P	q	P	q
kPa	mol·kg^{-1}	kPa	mol·kg^{-1}	kPa	mol·kg^{-1}
111.864	0.024	122.837	0.021	123.226	0.021
222.785	0.085	222.802	0.044	227.066	0.036
346.448	0.106	325.643	0.064	344.167	0.056
463.186	0.126	457.285	0.087	464.898	0.083
573.074	0.162	574.316	0.110	615.309	0.107
755.186	0.275	933.319	0.182	1049.997	0.185
941.146	0.364	1196.939	0.241	1296.565	0.232
1222.887		1513.418	0.305	1570.848	0.279
D		D		D	
0.0408		0.0242		0.0214	

Prior to introduction of adsorbate into the reaction cell, the adsorbent mass was weighed within ±10 mg accuracy after eliminating impurity traces at 423.15 K and high vacuum for more than 12 h. After the adsorbent was placed in the reaction cell, the impurity traces in the reaction cell were eliminated by vacuum pump for 3 h, similar to the case of the loading cell. When the temperatures in the loading and the reaction cells attained required levels, the experiment was initiated. First, the adsorbate was introduced into the loading cell, and then when the temperature and pressure in the loading cell stabilized, the valve between the loading and reaction cells was opened. The adsorption equilibrium state was considered to be when the temperatures and the pressures per cell were constant. Temperatures and pressures before and after the adsorption equilibrium state were recorded. The experiment was conducted, on a continuous basis, at pressures up to 2 MPa. The amount adsorbed was calculated, from the temperature and pressure, before and after the adsorption equilibrium state using the mass balance given by eq 1.

$$\frac{PV}{ZRT}\Big|_{l_1} + \frac{PV}{ZRT}\Big|_{a_1} = \frac{PV}{ZRT}\Big|_{l_2} + \frac{PV}{ZRT}\Big|_{a_2} + qM \qquad (1)$$

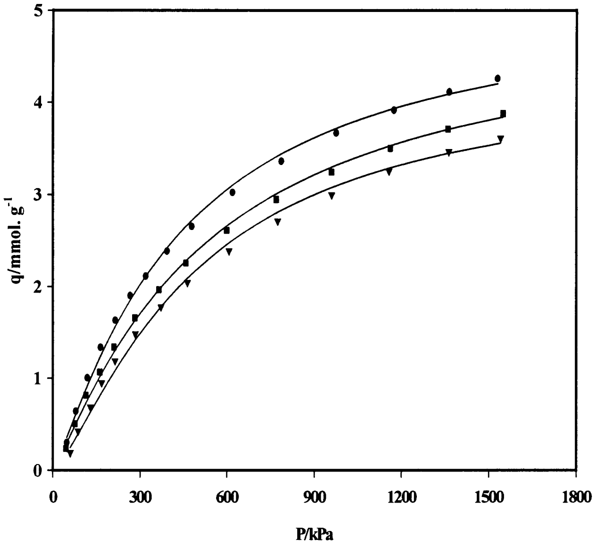

Figure 2. Measured and fitted isotherms of CH_4 onto activated carbon: ●, 293.15 K; ■, 303.15 K; ▼, 313.15 K; —, L−F model.

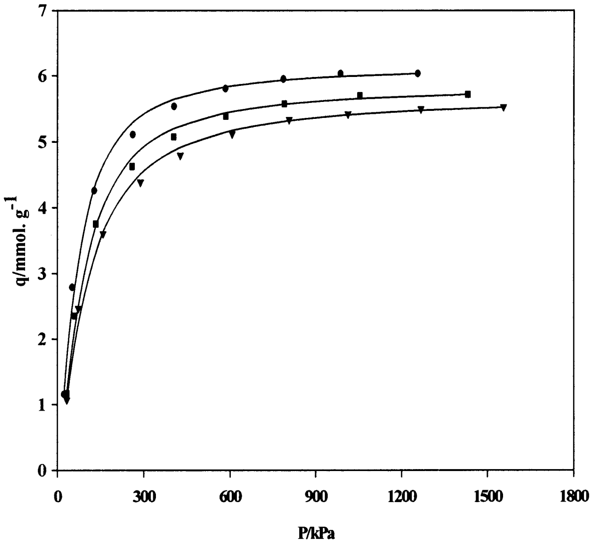

Figure 3. Measured and fitted isotherms of C_2H_6 onto activated carbon: ●, 293.15 K; ■, 303.15 K; ▼, 313.15 K; —, L−F model.

in which P is pressure, T is temperature, V is volume, R is the gas constant, M is the molecule weight, Z is the compressibility factor, and q is the amount adsorbed. 1 represents the state prior to the adsorption equilibrium; 2, the final equilibrium state.

Results and Discussion

The adsorption data for methane, ethane, ethylene, hydrogen, and nitrogen onto activated carbon adsorbent were obtained at 293.15 K, 303.15 K, and 313.15 K and pressures up to 2 MPa. The experimental data are represented in Tables 2−6 and are graphically presented in Figures 2−6. In these figures, solid lines represent the experimental data.

The methane, ethane, ethylene, hydrogen, and nitrogen adsorption isotherms resembled the Langmuir isotherm classified as type-I according to Brunauer et al.[15] This type is characterized by stronger attractive forces between the adsorbate and adsorbent than between the molecules of the adsorbate in the bulk state.[1] In other words, the pore size of the adsorbent is not very much greater than the molecular diameter of the adsorbate molecule.

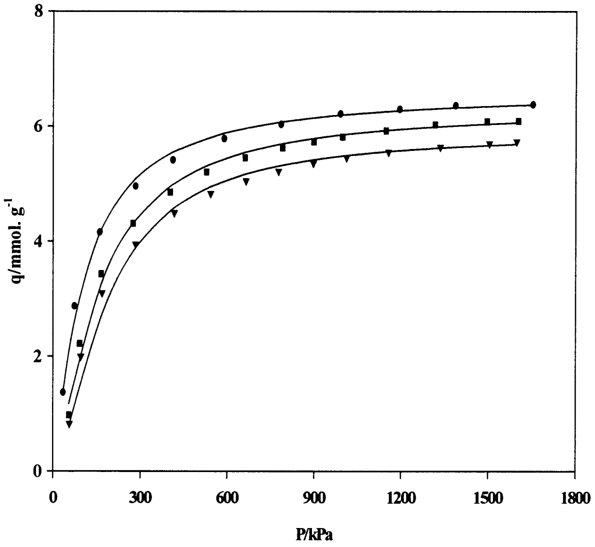

Figure 4. Measured and fitted isotherms of C_2H_4 onto activated carbon: ●, 293.15 K; ■, 303.15 K; ▼, 313.15 K; —, L−F model.

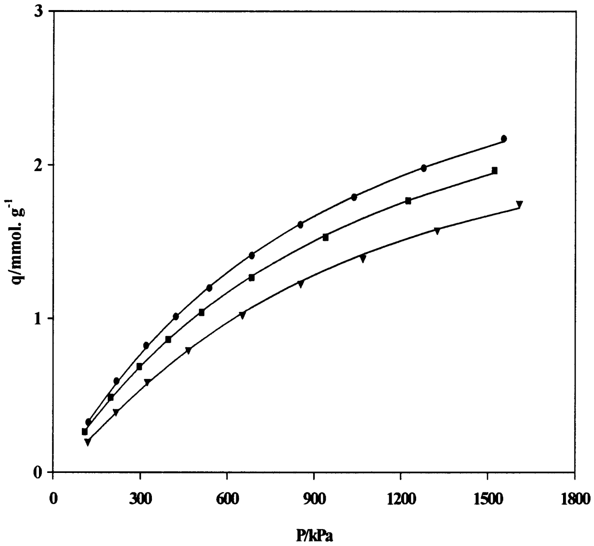

Figure 5. Measured and fitted isotherms of N_2 onto activated carbon: ●, 293.15 K; ■, 303.15 K; ▼, 313.15 K; —, L−F model.

For each equilibrium datum, rigorous assessments were performed and correlated by several pure species equilibrium models. The isotherm equations used in this study were Langmuir,[1] Freundlich,[1] Langmuir−Fruendlich,[1] Toth,[16] and Unilan.[16] The mathematical forms of these models are as follows:

Langmuir
$$q = \frac{q_m B P}{1 + BP} \tag{2}$$

Freundlich
$$q = kP^{1/t} \tag{3}$$

Langmuir−Freundlich
$$q = \frac{q_m B P^{1/t}}{1 + BP^{1/t}} \tag{4}$$

Toth
$$q = \frac{q_m P}{(B + P^t)^{1/t}} \tag{5}$$

Unilan
$$q = \frac{q_m}{2s} \ln\left[\frac{c + P\exp(+s)}{c + P\exp(-s)}\right] \tag{6}$$

where q is the amount adsorbed, P is the equilibrium pressure, and q_m, B, k, t, c, and s are isotherm parameters.

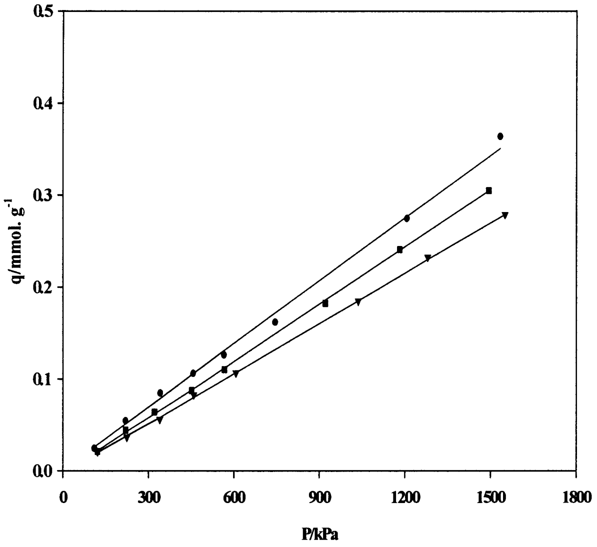

Figure 6. Measured and fitted isotherms of H_2 onto activated carbon: ●, 293.15 K; ■, 303.15 K; ▼, 313.15 K; —, L−F model.

To find the isotherm parameters for each adsorption system, two parameter estimation techniques were applied. These methods include a least-squares fitting method, which correlated the Langmuir, Freundlich, and Langmuir−Freundlich equations, and the so-called Nelder−Mead simplex pattern search algorithms, which correlated the Toth and the Unilan equations. In addition, the following objective functions were used in this study,

$$\min \sum_j (N_j^{\text{obs}} - N_j^{\text{cal}})^2 \tag{7}$$

where N_j^{obs} are the experimental data of the amount adsorbed and N_j^{cal} are the correlation results. Also, the deviation parameter on the amount adsorbed, *D*, was utilized to compare the correlation results with experimental data,

$$D = \frac{1}{n}\sum_i^n \left|\frac{N_i^{\text{obs}} - N_i^{\text{cal}}}{N_i^{\text{obs}}}\right| \tag{8}$$

where *n* is the number of data. The average deviation parameters for each component were represented in Tables 2−6.

For all the systems, the isotherms showed nonlinearity, except for hydrogen. One of the main reasons for isotherm nonlinearity stems from adsorbent surface heterogeneity. This is generally the case for activated carbon. Also, surface heterogeneity depends on the relative sizes of the adsorbate and active sites.[14] The amount adsorbed of methane, ethane, and ethylene increased significantly at low pressure, under 0.3 MPa. Especially, at the same pressure and temperature, the adsorbed amount of ethane and ethylene is always higher than that for methane, due to the higher polarizability of the ethane and ethylene molecule. For nitrogen, the behavior is observed to be similar.

The Langmuir−Freundlich equation was used for all the systems because this equation showed the minimum value of the average deviation parameter. Since the Langmuir−Freundlich isotherm has three adjustable parameters, it usually gave a more accurate correlation than the Langmuir and Fruendlich isotherms, both of which have only two adjustable parameters. Although the Toth and the Unilan equations predicted well experimental data at low pressure, they did not predict well at high pressure, because they obey Henry's law at low pressure but the adsorbed amount approaches saturating loading at high pressure. Additionally, the L−F model is certainly superior to the others. The computational load is evidently crucial, besides the model accuracy, since the ultimate goal of this study is to determine an appropriate model to develop a PSA simulation model.[14] In other words, for multicomponent equilibria, the simpler extended versions of the single-component models provide an adequate and numerically convenient means of predictions.[14] The isotherm parameters for the Langmuir−Freundlich equation were given in Table 7.

Isosteric enthalpies of adsorption can be calculated by the Clausius−Clapeyron equation[17] applied to adsorption,

$$\frac{q_{\text{st}}}{RT^2} = \left[\frac{\partial \ln P}{\partial T}\right]_q \tag{9}$$

where *P* is pressure, *T* is temperature, *R* is the gas constant, and q_{st} is the isosteric enthalpy.

The isosteric enthalpy is a measure of the interaction between adsorbate molecules and adsorbent lattice atoms and may be used as a measure of the energetic heterogeneity of a solid surface. Usually, the isosteric enthalpy of adsorption varies with surface coverage. Therefore, the relation between isosteric enthalpy and coverage explains the surface structure.[17,18] For homogeneous surfaces, as coverage increases, lateral interactions increase; thus, the isosteric enthalpy of adsorption increases. Vertical interactions do not depend on coverage and are determined from limiting isosteric enthalpy at zero coverage.[18] Thus, the isosteric enthalpy versus surface coverage relation cannot be determined a prior for heterogeneous surfaces. However, a decreasing isosteric enthalpy with increasing surface coverage usually indicates a heterogeneous surface. A constant value would indicate either a homogeneous surface with no lateral interactions or a heterogeneous surface where the change in lateral interactions exactly cancels the change in vertical interactions.[17] According to the ideal Langmuir model, the enthalpy of adsorption should be independent of coverage, but this requirement is seldom fulfilled in real systems because the effects of surface heterogeneity and adsorbate−adsorbate interaction are generally significant.

As shown in Figure 7, the isosteric enthalpies of adsorption varied with the surface loading on activated carbon

Table 7. Langmuir−Fruendlich Adsorption Isotherm Parameters for CH_4, C_2H_6, C_2H_4, N_2, and H_2 onto Activated Carbon

	293.15 K			303.15 K			313.15 K		
	q_m	B		q_m	B		q_m	B	
adsorbate	mmol·g^{-1}	MPa^{-1}	t	mmol·g^{-1}	MPa^{-1}	t	mmol·g^{-1}	MPa^{-1}	t
CH_4	5.154	1.757	0.848	4.944	1.471	0.870	4.316	1.194	0.748
C_2H_6	6.148	16.600	0.737	5.837	11.685	0.722	5.681	9.662	0.771
C_2H_4	6.594	9.455	0.826	6.302	5.280	0.722	5.890	3.869	0.651
N_2	3.317	0.878	0.905	3.161	0.839	0.924	2.579	0.681	0.824
H_2	12.344	0.0197	0.995	10.146	0.0197	0.948	9.719	0.0197	0.954

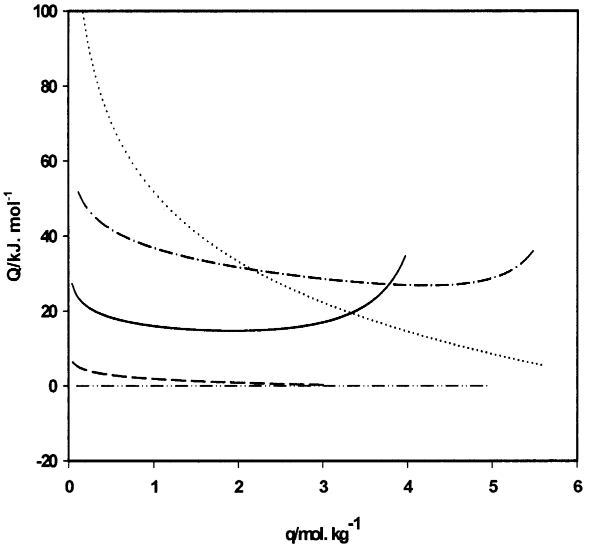

Figure 7. Isosteric enthalpy of adsorption with respect to surface loading onto activated carbon: —, CH_4; ···, C_2H_6; -·-, C_2H_4; - - -, N_2; -··-, H_2.

adsorbent. And, a strong adsorption energetic heterogeneity is commonly observed on such adsorbents as activated carbon.[10] This result indicates that the activated carbon adsorbents used have an energetically heterogeneous surface. For methane, ethane, and ethylene, the isosteric enthalpy of adsorption decreased and then increased. In other words, energetic heterogeneity's effect is the main effect at first, and then the interaction between adsorbate and adsorbate becomes the main effect with the amount adsorbed. Also, the interaction between the adsorbate and the adsorbent is increased with the increase in the number of carbons.

Conclusions

The adsorption equilibrium data of methane, ethane, ethylene, nitrogen, and hydrogen onto activated carbon adsorbent were obtained at 293.15 K, 303.15 K, and 313.15 K and pressures up to 2 Mpa. The experimental data of all components were correlated by the Langmuir-Freundlich equation, which showed remarkable quality assessments. The isosteric heats of adsorption were calculated by the Clausius–Clapeyron equation, allowing the conclusion that the activated carbon has an energetically heterogeneous surface.

Literature Cited

(1) Yang, R. T. *Gas Separation by Adsorption Processes*; Butterworth: Boston, MA, 1987.
(2) Ruthven, D. M. *Principles of Adsorption and Adsorption Processes*; John Wiley & Sons: New York, 1984.
(3) Costa, E.; Soreto, J. L.; Calleja, G.; Marron, C. Adsorption of Binary and Ternary Hydrocarbon Gas Mixtures on Activated Carbon: Experimental Determination and Theoretical Prediction of The Ternary Equilibrium Data. *AIChE J.* **1987**, 27, 5–12.
(4) Stewart, H. A.; Heck, J. L. Pressure Swing Adsorption. *J. Chem. Eng. Prog.* **1969**, *65*, 78–83.
(5) Yang, R. T.; Doong, S. J. Gas Separation by Pressure Swing Adsorption: A Pore-Diffusion Model for Bulk Separation. *AIChE J.* **1985**, *31*, 1829–1842.
(6) Park, J. H.; Kim, J. N.; Cho, S. H. Performance Analysis of Four-Bed H_2 PSA Process Using Layered Beds. *AIChE J.* **2000**, *46*, 790–802.
(7) Cen, P.; Yang, R. T. Bulk Gas Separation by Pressure Swing Adsorption. *Ind. Eng. Chem. Fundam.* **1986**, *25*, 758–767.
(8) Yang, J. Y.; Lee, C. H. Separation of Hydrogen Mixtures by a Two-Bed Pressure Swing Adsorption Process Using Zeolite 5A. *Ind. Eng. Chem. Res.* **1997**, *36*, 2789–2798.
(9) Ahmadpour, A.; Wang, K.; Do, D. D. Comparison of Models on the Predition of Binary Equilibrium Data of Activated Carbons. *AIChE J.* **1998**, *44*, 740–752.
(10) Shizhang, Q.; Kean, W.; Xijun, H. Study of Binary Adsorption Equilibrium of Hydrocarbons in Activated Carbon Using Micropore Size Distribution. *Langmuir* **2000**, *16*, 5130–5136.
(11) Kalu, B. K.; Sweed, N. H. *Fundamentals of Adsorption*; Eng. Foundation: New York, 1984.
(12) Myers, A. L.; Prausnitz, J. M. Thermodynamics of Mixed-Gas Adsorption. *AIChE J.* **1965**, *11*, 121–126.
(13) Suwanayuen, S.; Danner, R. P. A Gas Adsorption Isotherm Equation Based on Vacancy Solution Theory. *AIChE J.* **1980**, *26*, 68–76.
(14) Malek, A.; Farooq, S. Comparison of Isotherm Models for Hydrocarbon Adsorption on Activated Carbon. *AIChE J.* **1996**, *42*, 3191–3201.
(15) Brunauer, S.; Deming, L. S.; Deming, W. E.; Teller, E. J. On theory of The van der Waals Adsorption Gases. *J. Am. Chem. Soc.* **1940**, *62*, 1723–1732.
(16) Valenzuela, D. P.; Myers, A. L. *Adsorption Equilirium Data Handbook*; Prentice Hall: Englewood Cliffs, NJ, 1989.
(17) Hill, T. L. Statistical Mechanics of Adsorption. V. Thermodynamics and Heat of Adsorption. *J. Chem. Phys.* **1949**, *17*, 520–535.
(18) Ross, S.; Oliver, J. P. *On Physical Adsorption*; Wiley: New York, 1964.

Received for review August 21, 2002. Accepted February 3, 2003.

JE020161D